NIH Public Access
Author Manuscript
J Pathol. Author manuscript; available in PMC 2009 December 10.

Published in final edited form as:
J Pathol. 2009 September ; 219(1): 52–60. doi:10.1002/path.2566.

Bone loss in survival motor neuron (*Smn*$^{-/-}$*SMN2*) genetic mouse model of spinal muscular atrophy

Srinivasan Shanmugarajan[1], **Eichi Tsuruga**[1], **Kathryn J Swoboda**[3], **Bernard L Maria**[1], **William L Ries**[2], and **Sakamuri V Reddy**[1,*]

[1]Charles P. Darby Children's Research Institute, Charleston, SC, USA

[2]College of Dental Medicine, Medical University of South Carolina, Charleston, SC, USA

[3]Division of Neurology, Department of Pediatrics, University of Utah School of Medicine, Salt Lake City, UT, USA

Abstract

Spinal muscular atrophy (SMA) is characterized by degenerating lower motor neurons and an increased incidence of congenital bone fractures. Survival motor neuron (SMN) levels are significantly reduced due to deletions/mutations in the telomeric *SMN1* gene in these patients. We utilized the Smn$^{-/-}$ SMN2 mouse model of SMA to determine the functional role for SMN in bone remodelling. μCT analysis of lumber vertebrae, tibia and femur bones from SMA mice revealed an osteoporotic bone phenotype. Histological analysis demonstrated a thin porous cortex of cortical bone and thin trabeculae at the proximal end of the growth plate in the vertebrae of SMA mice compared to wild-type mice. Histochemical staining of the vertebrae showed the presence of abundant activated osteoclasts on the sparse trabeculae and on the endosteal surface of the thin cortex in SMA mice. Histomorphometric analysis of vertebrae from SMA mice showed an increased number of osteoclasts. Serum TRAcP5b and urinary NTx levels were elevated, consistent with increased bone resorption in these mice. SMA mice showed a significant decrease in the levels of osteoblast differentiation markers, osteocalcin, osteopontin and osterix mRNA expression; however, there were no change in the levels of alkaline phosphatase expression compared to WT mice. SMA mouse bone marrow cultures revealed an increased rate of osteoclast formation (54%) and bone resorption capacity (46%) compared to WT mice. Pre-osteoclast cells from SMA mice showed constitutive up-regulation of RANK receptor signalling molecules critical for osteoclast differentiation. Our results implicate SMN function in bone remodelling and skeletal pathogenesis in SMA. Understanding basic mechanisms of SMN action in bone remodelling may uncover new therapeutic targets for preventing bone loss/fracture risk in SMA.

Keywords

spinal muscular atrophy; osteoclast; RANK ligand; survival motor neuron; mouse model

Copyright © 2009 Pathological Society of Great Britain and Ireland. Published by John Wiley & Sons, Ltd.

*Correspondence to: Sakamuri V Reddy, Charles P. Darby Children's Research Institute, 173 Ashley Avenue, Charleston, SC 29425, USA. reddysv@musc.edu

No conflicts of interest were declared.

NIH-PA Author Manuscript
NIH-PA Author Manuscript
NIH-PA Author Manuscript

NIH-PA Author Manuscript

NIH-PA Author Manuscript

NIH-PA Author Manuscript

Introduction

Spinal muscular atrophy (SMA) is the second most common fatal autosomal recessive childhood disorder, with a frequency of 1 in 8000 newborns. The disease is primarily characterized by degeneration of lower motor neurons [1]. However, patients with SMA have been shown to have an increased incidence of congenital bone fractures and hypercalcaemia with hypercalciuria, thought to be caused by altered bone turnover [2-4]. SMA patients almost universally demonstrate osteopenia and an increased risk for bone fractures. Also, a severe SMA variant has been described with congenital bone fractures and extremely thin ribs but without contractures [2]. Recently, it has also been reported that bone mineral density (BMD) is normal in most young SMA patients. BMD decreased significantly with increasing age, indicating that factors other than decreased mobility account for altered BMD in older patients with SMA [5].

SMA determining gene encoding protein, survival motor neuron (SMN) levels are significantly reduced due to deletions/mutations in the telomeric *SMN1* gene in SMA patients. However, a centromeric copy of the *SMN2* gene cannot compensate for the deficiency, due to an aberrant splicing of the exon 7 region [6]. SMN expression is ubiquitous and it has been reported that the SMN oligomerization defect that results from increased expression of the SMN Δ7 correlates with the severity of the human SMA disease [7]. The mouse genome contains a single copy of *Smn*, which is equivalent to human *SMN1*. Mouse Smn has 82% homology with the human SMN protein and aberrant splicing of *SMN* Δ7 does not occur in mouse tissues because of the absence of *SMN2*, which is present in the human genome [8]. It has been shown that mice with homozygous *Smn* disruption display massive cell death during early embryonic development, indicating that the Smn protein is necessary for cell survival and normal function [9]. Furthermore, transgenic mice harbouring the human *SMN2* gene in the $Smn^{-/-}$ background ($Smn^{-/-}$ *SMN2*) showed pathological changes in the spinal cord and skeletal muscles, similar to human SMA [10,11]. *SMN2* gene expression in $Smn^{-/-}$ mice rescued embryonic lethality but the mice had SMA. Interestingly, dual-energy X-ray absorptiometry (DEXA) analysis identified $Smn^{-/-}$ *SMN2* mice with skeletal abnormalities and degeneration of the tail [12].

The osteoclast is the bone-resorbing cell derived from the monocyte/macrophage lineage. The tumor necrosis factor (TNF) family member, receptor activator of nuclear factor κB (RANK) ligand (RANKL) is expressed on marrow stromal/osteoblast cells in response to several osteotropic factors. RANKL is critical for osteoclast precursor differentiation to form multinucleated osteoclasts, which resorb bone. M-CSF is required for proliferation, survival and expression of RANK receptor in osteoclast precursors. The RANKL-RANK interaction results in activation of various signalling cascades during osteoclast development and bone resorption activity [13]. We have previously reported SMN protein interaction with osteoclast stimulatory factor (OSF) and a functional role for SMN in bone resorbing human osteoclasts in bone marrow cultures [14]. These studies implicate a potential role for SMN in skeletal pathology in SMA. In this study, we utilized the $Smn^{-/-}$ *SMN2* mouse model of SMA to determine the functional role for SMN in bone remodelling.

Materials and methods

$Smn^{-/-}$ *SMN2* mice

SMA transgenic mice harbouring the human *SMN2* gene in the $Smn^{-/-}$ background ($Smn^{-/-}$ *SMN2*) [10] were obtained from the Jackson laboratory (Bar Harbor, ME, USA).

NIH-PA Author Manuscript

NIH-PA Author Manuscript

NIH-PA Author Manuscript

Microcomputed tomography (μCT) analysis

The bone samples from wild-type (WT) and SMA mice (4 weeks old) were dissected of soft tissues, fixed in 70% ethanol and the distal metaphysis scanned with a Skyscan 1072 μCT instrument (Skyscan, Antwerp, Belgium). μCT-Analyser software (from SkyScan) was used to analyse the structure of the sample, using the global segmentation method. Two-dimensional (2D) images were used to generate three-dimensional (3D) reconstructions and to calculate morphometric parameters with the 3D creator software supplied with the instrument.

Histological and histomorphometric analysis

The wild-type (WT) and SMA mouse lumber vertebrae were fixed in 4% paraformaldehyde in phosphate-buffered saline (PBS), decalcified in 0.5 M EDTA, pH 7.4, for 1–3 weeks and processed for paraffin embedding. Serial 5 μm sections were stained with haematoxylin and eosin (H&E). For histomorphometric analysis, 4% paraformaldehyde-fixed bone samples were dehydrated with serial changes in 70–100% ethanol. The specimens were embedded in methylmethacrylate (MMA). Serial 4–6 μm sections of MMA-GMA embedded tissues were stained for tartrate-resistant acid phosphatase (TRAP) activity, using a histochemical kit (Sigma Chemical Corp, MO, USA) as described [15,16]. Histomorphometric analysis was performed using OsteoMeasure version 2.2 software (Osteometrics, Atlanta, GA, USA). The specimens were analysed for the number of osteoclasts per bone perimeter (N.OCL/B.pm).

Osteoclast precursor (CFU-GM) culture

Non-adherent mononuclear cells from WT and SMA mouse bone marrow were cultured in methyl cellulose to form CFU-GM, as described previously [17]. Briefly, the non-adherent bone marrow cells (4×10^5/ ml) were cultured in Methocult H4230 (Stem Cell Technologies Inc., WA, USA) and incubated for 7 days. Cultures were scored for colonies (aggregates > cells) using an Olympus dissecting microscope (Olympus Optical Co., Tokyo, Japan). The results are reported as mean ± SD for quadruplicate cultures.

Osteoclast formation and bone resorption assay

Wild-type (WT) and SMA mouse bone marrow cells were cultured to form osteoclasts, as described [18]. Briefly, WT and SMA mouse bone marrow non-adherent cells (1.3×10^6/ ml) were cultured in 24-well plates for 4–5 days in the presence of mRANKL (5–100 ng/ml) and mM-CSF (10 ng/ml). Cells were fixed in 2% glutaraldehyde in PBS for 20 min and stained for TRAP activity. TRAP-positive MNCs containing three or more nuclei were scored under a microscope. Bone resorption activity of the osteoclasts was assayed by culturing the WT and SMA mouse bone marrow cells in the presence of RANKL (100 ng/ml) and M-CSF (10 ng/ml) for 10 days on dentine slices. At the end of the culture period, adherent cells were removed from the dentine disc, using 1 M NaOH, and stained with 0.1% toluidine blue. The bone resorption area was quantified using computerized image analysis (Adobe Photoshop and Scion MicroImaging version β4.2). The percentage of the resorbed area was calculated relative to the total dentine disc area.

Real-time RT-PCR analysis

The wild-type and SMA mouse bone marrow-derived stromal/preosteoblast cells were cultured with medium containing 10 mM β-glycerophosphate and 50 μg/ml ascorbic acid for 9 days, and total RNA (2 μg) was isolated using RNAzol reagent (Tel-Test Inc, Friendswood, TX, USA). A reverse-transcription reaction was performed using poly-dT primer and Moloney murine leukaemia virus reverse transcriptase (Applied Biosystems) in a 25 μl reaction volume containing total RNA (2 μg), 1× PCR buffer and 2 m M $MgCl_2$, at 42 °C for 15 min, followed by 95 °C for 5 min. The resulting cDNAs were subjected to real-time PCR analysis, using SYBR Green Supermix in an iCycler (iCycler iQ Single-color Real-time PCR detection system;

NIH-PA Author Manuscript

NIH-PA Author Manuscript

NIH-PA Author Manuscript

Bio-Rad, Hercules, CA, USA) for osteoblast differentiation markers, using gene-specific primers for: osteocalcin, sense 5′-TCTGACAAACCTTCATGTCC-3′ and antisense 5′-AAATAGTGATACCGTAGATGCG-3′; alkaline phosphatase, sense 5′-GCCCTCTCCAAGACATATA-3′ and antisense 5′-CCATGATCACGTCGATATCC-3′; osteopontin; sense 5′-TAGTGCCACAGATGAGGACCT-3′and antisense 5′-CAGAGGGCATGCTCAGAAGCT-3′; osterix, sense 5′-GGTCCAGGCAACACACCTAC-3′ and antisense 5′-GGTAGGGAGCTGGGTTAAGG-3′; RANKL, sense 5′-ACCAGCATCAAAATCCCAAG-3′and antisense 5′-TAAGGAGGGGTTGGAGACCT-3′; OPG, sense 5′-TCCTGGCACCTACCTAAAACAGCA-3′ and antisense 5′-CTACACTCTCGGCATTCACTTTGG-3′; GAPDH, sense 5′-CCTACCCCCAATGTATCCGTTGTG-3′ and antisense 5′-GGAGGAATGGGAGTTGCTGTTGAA-3′. Thermal cycling at 94 °C for 3 min, followed by 40 cycles of amplification at 94 °C for 30 s, 66 °C for 1 min, 72°C for 1 min and 72 °C for 5 min as the final elongation step. Relative levels of mRNA expression were normalized in all the samples analysed with respect to the levels of *GAPDH* amplification.

Biochemical assays

The osteoclast activity markers, serum bone-specific tartrate-resistant acid phosphatase 5b (TRAcP 5b) and urinary N-telopeptide (NTx) levels were measured in WT and SMA mice by ELISA, as described [18]. Serum calcium levels were measured using a QuantiChrom calcium assay kit (DICA-500), in which phenolsulphonephthalein dye forms a stable blue-coloured complex specifically with free calcium. The intensity of the colour is measured at 612 nm by a spectrophotometer, according to the manufacturer's protocol (BioAssay Sytems, CA, USA).

Western blot analysis

WT and SMA mouse bone marrow cells were resuspended in 10 ml α-MEM containing 10% FCS and mM-CSF (10 ng/ml) for 12 h. The non-adherent cells (1.5×10^6/ ml) obtained were treated with fresh α-MEM containing 10% FCS, 10 ng/ml mM-CSF and with or without 100 ng/ml mRANKL for 48 h. Total cell lysates obtained from these pre-osteoclast cells were subjected to Western blot analysis for RANK receptor signalling molecules (TRAF2, TRAF6, c-Fos, c-Jun).

p-c-Jun kinase activity assay

The non-adherent bone marrow cells (1.5×10^6/ ml) obtained from WT and SMA mice were cultured with fresh α-MEM containing 10% FCS, 10 ng/ml mM-CSF and with or without 100 ng/ml mRANKL stimulation for 15 min, and p-c-Jun kinase activity was performed as described earlier [19].

Statistical analysis

Data were presented as means and the statistical analysis between the WT and SMA mice for a given parameter was established by Student's *t*-test; values at $p < 0.05$ were considered statistically significant. Statistical analysis of skeletal parameters was also applied by one-way ANOVA.

Results

Low bone mineral density in SMA mice

Recently, it has been reported that children with SMA have low bone mineral density (BMD) [20]. Consistently, we have also shown poorly developed vertebrae in *Smn*$^{-/-}$ *SMN2* mice by DEXA analysis and a significant decrease in total bone density in these mice compared to wild-

NIH-PA Author Manuscript

NIH-PA Author Manuscript

NIH-PA Author Manuscript

type (WT) mice [12]. Here in, we further examine the 3D μCT images of lumbar vertebrae 1–3 dissected from SMA mice aged 4 weeks. Vertebrae from SMA mice showed a significant decrease in the percentage of bone volume (BV/TV), bone surface density (BS/TV) and trabecular number (Th.N) compared to WT mice (Figure 1A). Similarly, μCT images showed a significant decrease in bone volume (33%), bone surface density (35%) and trabecular number (50%) in the tibia and a decrease in bone volume (30%), bone surface density (19%) and trabecular number (30%) in the femur of SMA mice compared to WT mice (Figure 1B, C).

We also analysed the bone structure of vertebral bodies from SMA mice by histochemical staining. Histological analysis of sections from the lumbar vertebrae of WT mice stained with H&E showed wide dense cortical bone and coarse trabeculae. In contrast, SMA mouse vertebrae demonstrated thin porous cortical bone and fine trabeculae when compared to WT mice (Figure 2A). WT vertebrae showed TRAP activity-stained osteoclasts mostly confined to the primary spongiosa at the base of the growth plate, where mineralized cartilage would undergo resorption. In contrast, SMA mouse lumbar vertebrae showed increased numbers of TRAP-positive osteoclasts along the base of the growth plate as well as activity on most of the sparse trabeculae and on the endosteal surface of the thin cortex (Figure 2B). Bone histomorphometric analyses identified a significant increase (57.14%) in the osteoclast number per bone perimeter in the SMA mice (Figure 2C). These results indicated an osteoporotic bone phenotype in SMA.

High bone turnover in SMA mice

We next examined the status of biochemical markers of bone metabolism in SMA mice compared to WT mice. Biochemical analysis of osteoclast activity markers, such as serum TRAcP5b and urinary N-telopeptide (NTx) levels, were determined. ELISA analysis demonstrated a significant increase (64.2%) in the serum TRAcP5b levels and an 11-fold increase in urine NTx levels in SMA mice compared to WT mice (Figure 3A, B). Also, SMA mice showed an increased serum calcium level (41.6%) compared to WT mice (Figure 3C). We further examined the status of osteoblast differentiation markers in SMA mice. Wild-type (WT) and SMA mouse bone marrow-derived stromal/preosteoblast cells were cultured with medium containing 10 m_M β-glycerophosphate and 50 μg/ml ascorbic acid for 9 days. Total RNA (2 μg) isolated from these cells was subjected to real-time PCR analysis, using gene-specific primers for alkaline phosphatase, osteopontin, osterix, osteocalcin, osteoprotegerin (OPG) and RANKL. We found no significant change in the levels of *RANKL* and *OPG*, critical parameters that determine osteoclast development and bone mineral density in SMA mice. Also, there was no significant change in the mRNA expression levels of alkaline phosphatase, which is an early osteoblast differentiation marker (Figure 3D-F). However, the osteoblast mineral matrix markers osteoclacin, osteopontin and osterix levels were significantly decreased (48%, 74.5% and 20% respectively) in SMA mice compared to WT mice.

Enhanced osteoclast formation/bone resorption in SMA mouse bone marrow cultures

CFU-GM is the early osteoclast precursor and increased numbers of CFU-GM in pathological conditions resulted in increased osteoclast formation [21]. We therefore examined SMA mouse bone marrow cells for osteoclast precursor growth in methyl cellulose cultures. WT and SMA mouse bone marrow-derived non-adherent cells were cultured in methyl cellulose with GM-CSF (10 ng/ml) to form CFU-GM colonies, as described in Materials and methods. We found no significant difference in the number of CFU-GM colonies formed in SMA mouse bone marrow cultures compared to WT mice (Figure 4A). These results indicate that SMN deficiency has no significant effect on early osteoclast precursor cells. We then determined the capacity for osteoclast differentiation and bone resorption activity in bone marrow cultures. SMA- and WT mice-derived non-adherent bone marrow cells were stimulated with various concentrations

NIH-PA Author Manuscript

NIH-PA Author Manuscript

NIH-PA Author Manuscript

of RANKL (5–100 ng/ml) with M-CSF (10 ng/ml), and the number of TRAP-positive multinucleated osteoclasts formed in these cultures were scored. The number of osteoclasts formed in SMA mouse bone marrow cultures was significantly increased (54%) compared to control mice in response to RANKL (100 ng/ml) treatment (Figure 4B). We further examined the bone resorption capacity of osteoclasts formed in SMA mouse bone marrow cultures. Osteoclasts formed in SMA mouse bone marrow cultures demonstrated a significant increase (46%) in resorption area on dentine slices compared to WT mice when cultured in the presence of M-CSF (10 ng/ml) and RANKL (100 ng/ml) (Figure 4C). Taken together, these results suggest that SMA mice have high bone turnover with an increased osteoclast formation and bone resorption.

RANK receptor signalling in SMA mouse pre-osteoclast cells

RANKL-RANK signalling plays a critical role in osteoclast differentiation and bone resorption activity [22]. Therefore, we further examined the status of RANK receptor signalling molecules, such as TRAF2, TRAF6, c-Fos and c-Jun expression in pre-osteoclast cells. Non-adherent bone marrow cells derived from the WT and SMA mice were stimulated with and without RANKL (100 ng/ml) in the presence of M-CSF (10 ng/ml) for a 48 h period. Western blot analysis of total cell lysates obtained from SMA mice-derived pre-osteoclast cells revealed constitutive up-regulation of RANK, TRAF6, c-Fos and c-Jun expression; however, there were no significant change in the levels of TRAF2 expression. Further, TRAF6 expression was significantly increased (five-fold) in pre-osteoclast cells from SMA mice compared to WT mice in response to RANKL stimulation. Also, SMA mouse-derived preosteoclasts demonstrated a three-fold increase in the levels of c-Fos and c-Jun expression (Figure 5A). Further, SMA mouse preosteoclasts stimulated with RANKL for 30 min showed a significant increase in the levels of p-c-Jun kinase activity (Figure 5B). These results suggest that constitutive up-regulation of RANK receptor signalling molecules enhanced osteoclast formation and bone resorption activity in SMA mice.

Discussion

Skeletal complications of SMA include congenital bone fractures and osteopenia [20]. However, one of the unanswered questions in SMA has been whether bone pathology is only secondary to neurological dysfunction and disuse atrophy, or whether the skeleton phenotype in SMA is abnormal because of altered gene expression. In this study, μCT and histochemical analysis revealed an osteoporotic bone phenotype in SMA mice, with increased numbers of osteoclasts, thin cortices and decrease number of trabeculae. Osteoporosis is a well-known complication from immobility and unloading of the skeleton in disorders affecting the central nervous system, such as cerebral palsy or spinal cord injury [23]. However, our findings that the level of the bone turnover marker, urinary N-teleopeptide (NTx), is elevated in SMA mice cannot be explained by immobility and neurogenic atrophy. Therefore, it is unlikely that the bone phenotype in SMA could be a secondary consequence of muscle wasting. In fact, elevated urinary NTx levels are used as a biomarker for bone resorption and monitored during antiresorptive therapy with bisphosphonates and denosumab antibodies [24]. SMA mice-derived preosteoblast cells did not show significant change in the levels of alkaline phosphatase expression, indicating that osteoblast proliferation is not affected; however, low-level expression of mineral matrix markers such as osteocalcin and osteopontin is consistent with low BMD in patients with SMA, as reported [20].

We previously characterized SMA disease as determining *SMN* gene expression and differential splicing during osteoclast differentiation [14]. *SMN* expression is ubiquitous and SMN protein interacts with Bcl-2 to prevent Bax-induced or Fas-mediated apoptosis, although SMN itself had only weak anti-apoptotic activity [25]. Our results show that lack of significant

NIH-PA Author Manuscript

NIH-PA Author Manuscript

NIH-PA Author Manuscript

change in osteoclast precursor (CFU-GM) growth in SMA mouse bone marrow cultures does not implicate the anti-apoptotic function of SMN in osteoclast lineage cells. In SMA mice, we identified constitutive up-regulation of RANK and TRAF6 signalling molecules and enhanced levels of c-Jun kinase activity in preosteoclast cells responsible for increased rate of osteoclast differentiation and bone-resorbing activity.

Recently we reported that SMN interacts with specific signalling molecules, such as osteoclast stimulatory factor (OSF), which enhances osteoclast formation and bone-resorbing activity [14]. Further, SMN protein interactions include transcription factor E2 for upstream (FUSE) binding protein and tumour suppressor protein, p53 [26-28]. Therefore, it is likely that SMN affects osteoclast formation/bone resorption activity through modulation of RANK receptor signalling in preosteoclast cells. However, it is unclear that SMN protein interactions and functions are affected by the low SMN levels in SMA patients or in the SMA mouse model. Therefore identification and characterization of SMN protein interactions in osteoclasts may provide insights into novel signalling cascades that stimulate osteoclast formation/bone resorbing activity.

Taken together, our data indicate that SMN has a functional role in bone remodelling and that bone defects in patients with SMA cannot be fully explained by progressive anterior horn cell loss and neurogenic atrophy. Thus, studies pertaining to SMN function in bone cells may provide insights into the severe osteopenia and increased fracture risk often associated with SMA, and may identify novel targets for therapeutic interventions against bone loss to enhance quality of life in patients with SMA.

Acknowledgments

This work was conducted in a facility constructed with support from the National Institutes of Health (Grant No. C06 RR015455) from the Extramural Research Facilities Program of the National Center for Research Resources.

References

1. Swoboda KJ, Prior TW, Scott CB, McNaught TP, Wride MC, Reyna SP, et al. Natural history of denervation in SMA: relation to age, *SMN2* copy number, and function. Ann Neurol 2005;57:704–712. [PubMed: 15852397]
2. Felderhoff-Mueser U, Grohmann K, Harder A, Stadelmann C, Zerres K, Buhrer C, et al. Severe spinal muscular atrophy variant associated with congenital bone fractures. J Child Neurol 2002;17:718–721. [PubMed: 12503654]
3. Kelly TE, Amoroso K, Ferre M, Blanco J, Allinson P, Prior TW. Spinal muscular atrophy variant with congenital fractures. Am J Med Genet 1999;87:65–68. [PubMed: 10528250]
4. Khawaja K, Houlsby WT, Watson S, Bushby K, Cheetham T. Hypercalcaemia in infancy; a presenting feature of spinal muscular atrophy. Arch Dis Child 2004;89:384–385. [PubMed: 15033855]
5. Kinali M, Banks LM, Mercuri E, Manzur AY, Muntoni F. Bone mineral density in a paediatric spinal muscular atrophy population. Neuropediatrics 2004;35:325–328. [PubMed: 15627939]
6. Le TT, Pham LT, Butchbach ME, Zhang HL, Monani UR, Coovert DD, et al. SMNDelta7, the major product of the centromeric survival motor neuron (*SMN2*) gene, extends survival in mice with spinal muscular atrophy and associates with full-length *SMN*. Hum Mol Genet 2005;14:845–857. [PubMed: 15703193]
7. Lorson CL, Strasswimmer J, Yao JM, Baleja JD, Hahnen E, Wirth B, et al. SMN oligomerization defect correlates with spinal muscular atrophy severity. Nat Genet 1998;19:63–66. [PubMed: 9590291]DOI: 10.1038/ng0598-63
8. Bergin A, Kim G, Price DL, Sisodia SS, Lee MK, Rabin BA. Identification and characterization of a mouse homologue of the spinal muscular atrophy-determining gene, survival motor neuron. Gene 1997;204:47–53. [PubMed: 9434164]

NIH-PA Author Manuscript

NIH-PA Author Manuscript

NIH-PA Author Manuscript

9. Schrank B, Gotz R, Gunnersen JM, Ure JM, Toyka KV, Smith AG, et al. Inactivation of the survival motor neuron gene, a candidate gene for human spinal muscular atrophy, leads to massive cell death in early mouse embryos. Proc Natl Acad Sci USA 1997;94:9920–9925. [PubMed: 9275227]
10. Hsieh-Li HM, Chang JG, Jong YJ, Wu MH, Wang NM, Tsai CH, et al. A mouse model for spinal muscular atrophy. Nat Genet 2000;24:66–70. [PubMed: 10615130]
11. Monani UR, Sendtner M, Coovert DD, Parsons DW, Andreassi C, Le TT, et al. The human centromeric survival motor neuron gene (SMN2) rescues embryonic lethality in Smn−/− mice and results in a mouse with spinal muscular atrophy. Hum Mol Genet 2000;9:333–339. [PubMed: 10655541]
12. Shanmugarajan S, Swoboda KJ, Iannaccone ST, Ries WL, Maria BL, Reddy SV. Congenital bone fractures in spinal muscular atrophy: functional role for SMN protein in bone remodeling. J Child Neurol 2007;22:967–973. [PubMed: 17761651]
13. Reddy SV. Regulatory mechanisms operative in osteoclasts. Crit Rev Eukaryot Gene Expr 2004;14:255–270. [PubMed: 15663356]
14. Kurihara N, Menaa C, Maeda H, Haile DJ, Reddy SV. Osteoclast-stimulating factor interacts with the spinal muscular atrophy gene product to stimulate osteoclast formation. J Biol Chem 2001;276:41035–41039. [PubMed: 11551898]
15. Horn DA, Garrett IR. A novel method for embedding neonatal murine calvaria in methyl methacrylate suitable for visualizing mineralization, cellular and structural detail. Biotech Histochem 2004;79:151–158. [PubMed: 15621887]
16. Parfitt AM, Drezner MK, Glorieux FH, Kanis JA, Malluche H, Meunier PJ, et al. Bone histomorphometry: standardization of nomenclature, symbols, and units. Report of the ASBMR Histomorphometry Nomenclature Committee. J Bone Miner Res 1987;2:595–610. [PubMed: 3455637]
17. Koide M, Kurihara N, Maeda H, Reddy SV. Identification of the functional domain of osteoclast inhibitory peptide-1/hSca. J Bone Miner Res 2002;17:111–118. [PubMed: 11771657]
18. Shanmugarajan S, Irie K, Musselwhite C, Key LL Jr, Ries WL, Reddy SV. Transgenic mice with OIP-1/hSca overexpression targeted to the osteoclast lineage develop an osteopetrosis bone phenotype. J Pathol 2007;213:420–428. [PubMed: 17940999]
19. Koide M, Maeda H, Roccisana JL, Kawanabe N, Reddy SV. Cytokine regulation and the signaling mechanism of osteoclast inhibitory peptide-1 (OIP-1/hSca) to inhibit osteoclast formation. J Bone Miner Res 2003;18:458–465. [PubMed: 12619930]
20. Khatri IA, Chaudhry US, Seikaly MG, Browne RH, Iannaccone ST. Low bone mineral density in spinal muscular atrophy. J Clin Neuromuscul Dis 2008;10:11–17. [PubMed: 18772695]
21. Reddy SV, Menaa C, Singer FR, Demulder A, Roodman GD. Cell biology of Paget's disease. J Bone Miner Res 1999;14(suppl 2):3–8. [PubMed: 10510206]
22. Takayanagi H. Osteoimmunology: shared mechanisms and crosstalk between the immune and bone systems. Nat Rev Immunol 2007;7:292–304. [PubMed: 17380158]
23. Jiang SD, Jiang LS, Dai LY. Mechanisms of osteoporosis in spinal cord injury. Clin Endocrinol (Oxf) 2006;65:555–565. [PubMed: 17054455]
24. Geusens P, Reid D. Newer drug treatments: their effects on fracture prevention. Best Pract Res Clin Rheumatol 2005;19:983–989. [PubMed: 16301192]
25. Iwahashi H, Eguchi Y, Yasuhara N, Hanafusa T, Matsuzawa Y, Tsujimoto Y. Synergistic anti-apoptotic activity between Bcl-2 and SMN implicated in spinal muscular atrophy. Nature 1997;390:413–417. [PubMed: 9389483]
26. Young PJ, Day PM, Zhou J, Androphy EJ, Morris GE, Lorson CL. A direct interaction between the survival motor neuron protein and p53 and its relationship to spinal muscular atrophy. JBiol Chem 2002;277:2852–2859. [PubMed: 11704667]
27. Strasswimmer J, Lorson CL, Breiding DE, Chen JJ, Le T, Burghes AH, et al. Identification of survival motor neuron as a transcriptional activator-binding protein. Hum Mol Genet 1999;8:1219–1226. [PubMed: 10369867]
28. Williams BY, Hamilton SL, Sarkar HK. The survival motor neuron protein interacts with the transactivator FUSE binding protein from human fetal brain. FEBS Lett 2000;470:207–210. [PubMed: 10734235]

NIH-PA Author Manuscript
NIH-PA Author Manuscript
NIH-PA Author Manuscript

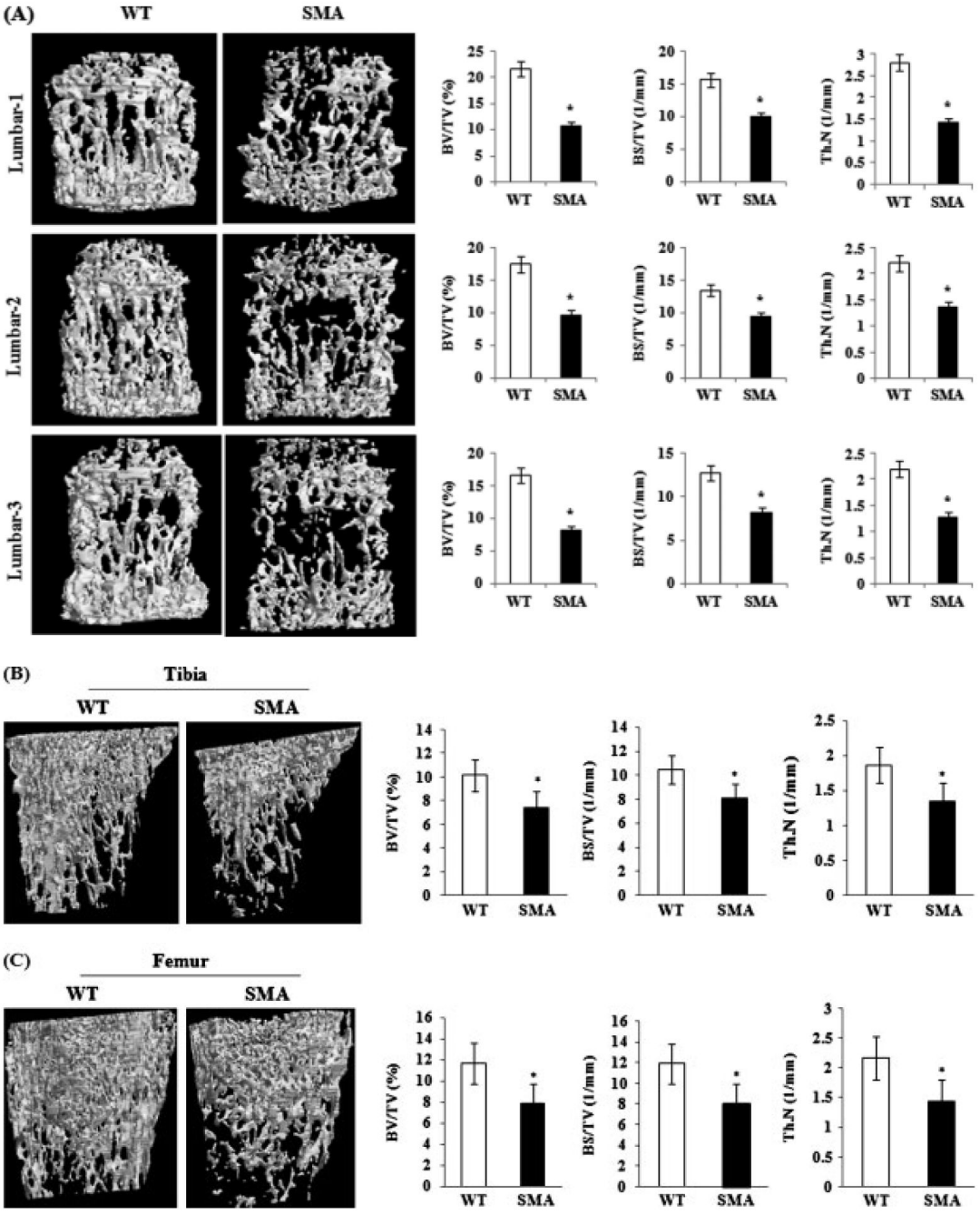

Figure 1.

μCT analysis of bones from wild-type (WT) and SMA mice. (A) 3D μCT images of lumbar vertebrae 1–3 dissected from 4 week-old mice. Quantification of μCT images showed a decrease in the percentage of bone volume (BV/TV), bone surface density (BS/TV) and trabecular number (Th.N) in the SMA mice compared to WT mice. (B) μCT images showed decreased bone mass of the tibia in SMA mice and the quantification showed decreased BV/TV, BS/TV and Th.N in SMA mice compared to WT mice. (C) μCT analysis of the femur from SMA mice compared to wild-type mice showed a decreased BV/TV, BS/TV and Th.N. The values represent mean ± SD ($n = 5$; $p < 0.05$)

NIH-PA Author Manuscript
NIH-PA Author Manuscript
NIH-PA Author Manuscript

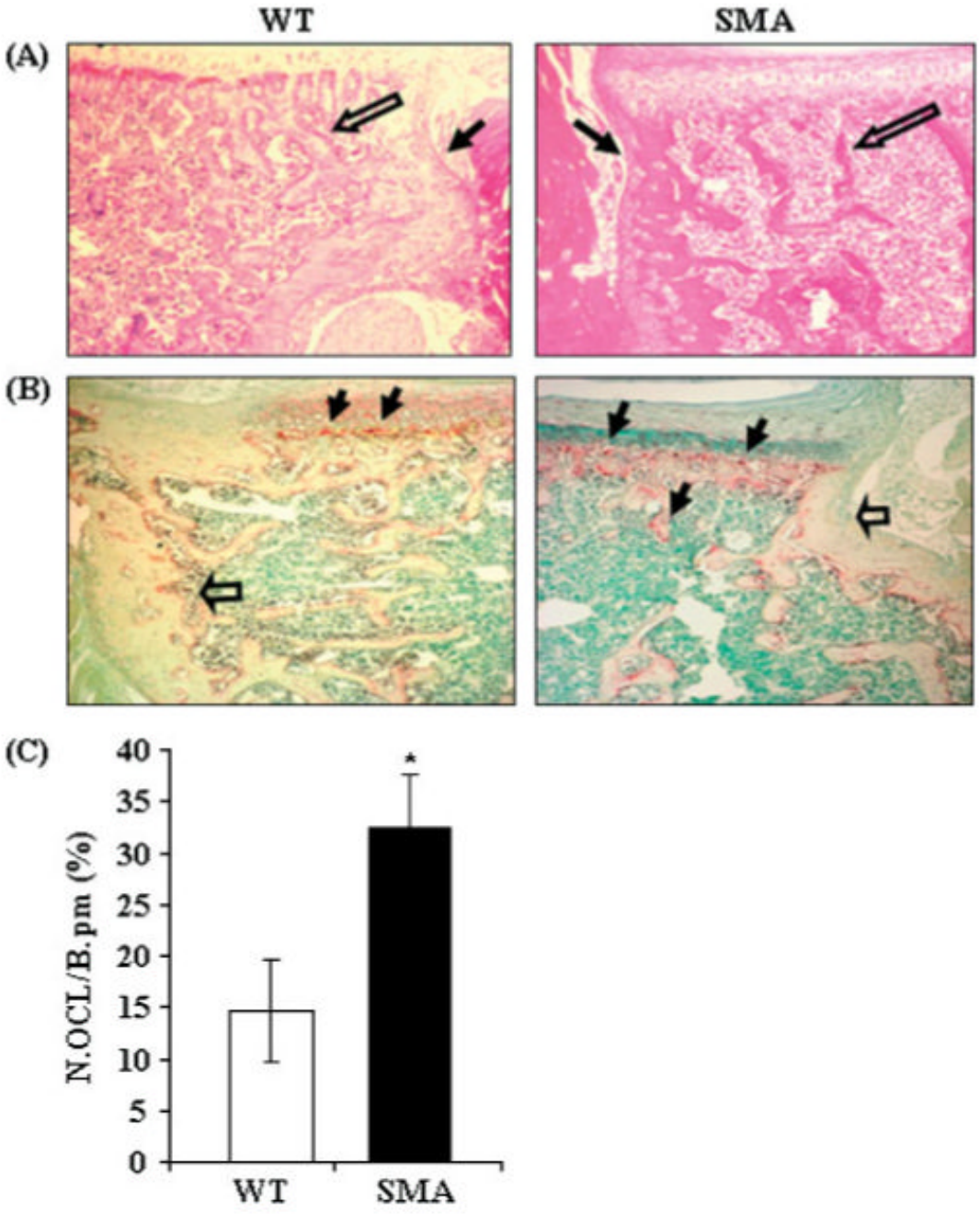

Figure 2.

Histological/histochemical analysis of wild-type (WT) and SMA mouse vertebrae. (A) WT vertebra showing a wide cortex of dense cortical bone (solid arrow) and coarse trabeculae (open arrow). SMA mouse vertebra show a thin porous cortical bone (solid arrow) and fine trabeculae (open arrow); H&E stain (×20). (B) WT vertebra showing TRAP-stained osteoclasts mostly confined to primary spongiosa at the base of growth plate (solid arrows). Note the wide cortex of dense cortical bone (open arrow) and coarse trabeculae with little TRAP staining. SMA mouse vertebra show increased numbers of TRAP-positive osteoclasts along the base of the growth plate as well as on most of the sparse trabeculae and on the endosteal surface of the relatively narrow cortex (open arrow). (C) Histomorphometric analysis of the number of

osteoclasts/bone perimeter (N.OCL/B.pm/100 mm). Values represent mean ± SD ($n = 5$; $p < 0.05$)

NIH-PA Author Manuscript
NIH-PA Author Manuscript
NIH-PA Author Manuscript

NIH-PA Author Manuscript
NIH-PA Author Manuscript
NIH-PA Author Manuscript

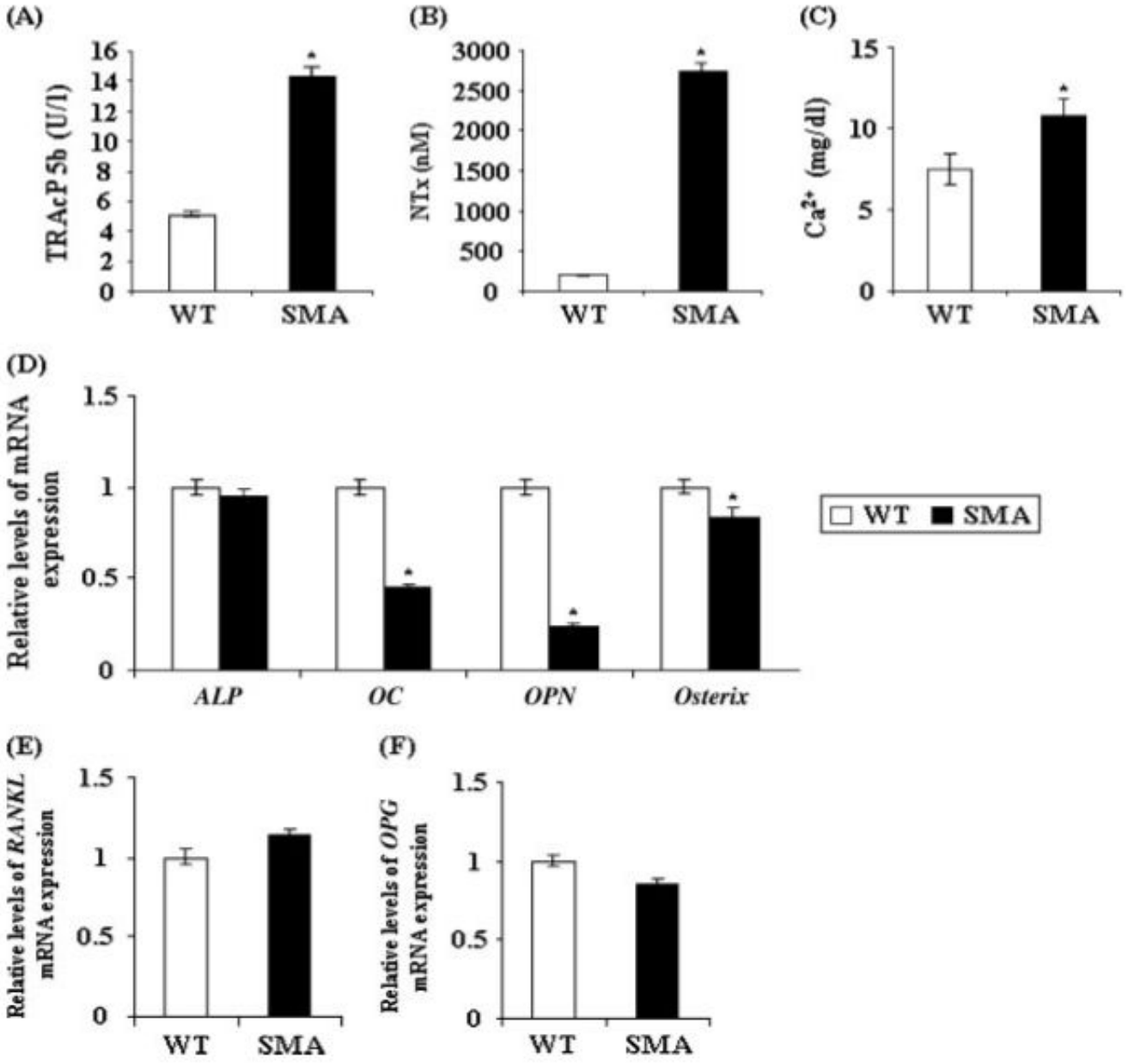

Figure 3.

Biochemical analysis of osteoclast activity and osteoblast differentiation markers in wild-type (WT) and SMA mice. (A) Serum TRAcP 5b. (B) Urine NTx levels were measured by ELISA. (C) Serum calcium levels. (D) Real-time PCR analysis of osteoblast markers (*ALP*, alkaline phosphatase; *OC*, osteocalcin; *OPN*, osteopontin; *Ox*, osterix). (E) *RANKL* mRNA expression. (F) *OPG* mRNA expression. The relative mRNA expression levels were normalized for *GAPDH* expression. The data represent three independent experiments ($p < 0.05$)

NIH-PA Author Manuscript
NIH-PA Author Manuscript
NIH-PA Author Manuscript

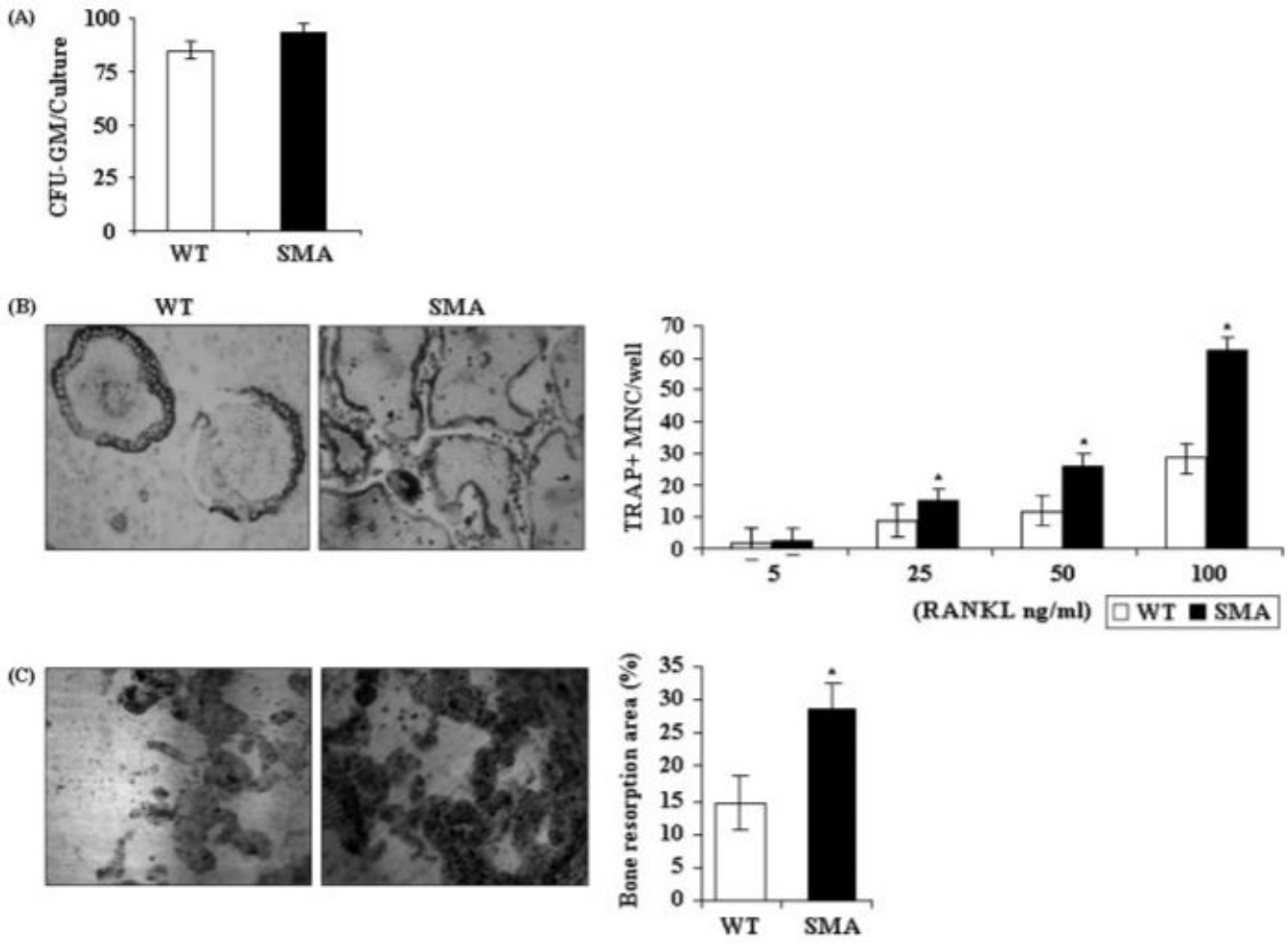

Figure 4.

Osteoclastogenesis in SMA mouse bone marrow cultures. (A) WT and SMA mouse-derived non-adherent cells (4×10^5/ ml) were cultured with hGM-CSF (10 ng/ml) in 1.2% methyl cellulose to form CFU-GM colonies. At the end of a 7 day culture period, CFU-GM colonies formed in these cultures were scored using a light microscope, as described in Materials and methods. (B) WT and SMA mouse bone marrow-derived non-adherent cells were stimulated with RANKL (5–100 ng/ml) and M-CSF (10 ng/ml) for 5 days and the $TRAP^+$ multinucleated cells (MNCs) formed in these cultures were scored. (C) WT and SMA mouse bone marrow-derived non-adherent cells (1×10^6/ml) were cultured to form osteoclasts on dentine slices. Resorption lacunae formed on dentine slices were quantified as described in Materials and methods. The results represent quadruplicate cultures of three independent experiments ($p < 0.05$)

NIH-PA Author Manuscript
NIH-PA Author Manuscript
NIH-PA Author Manuscript

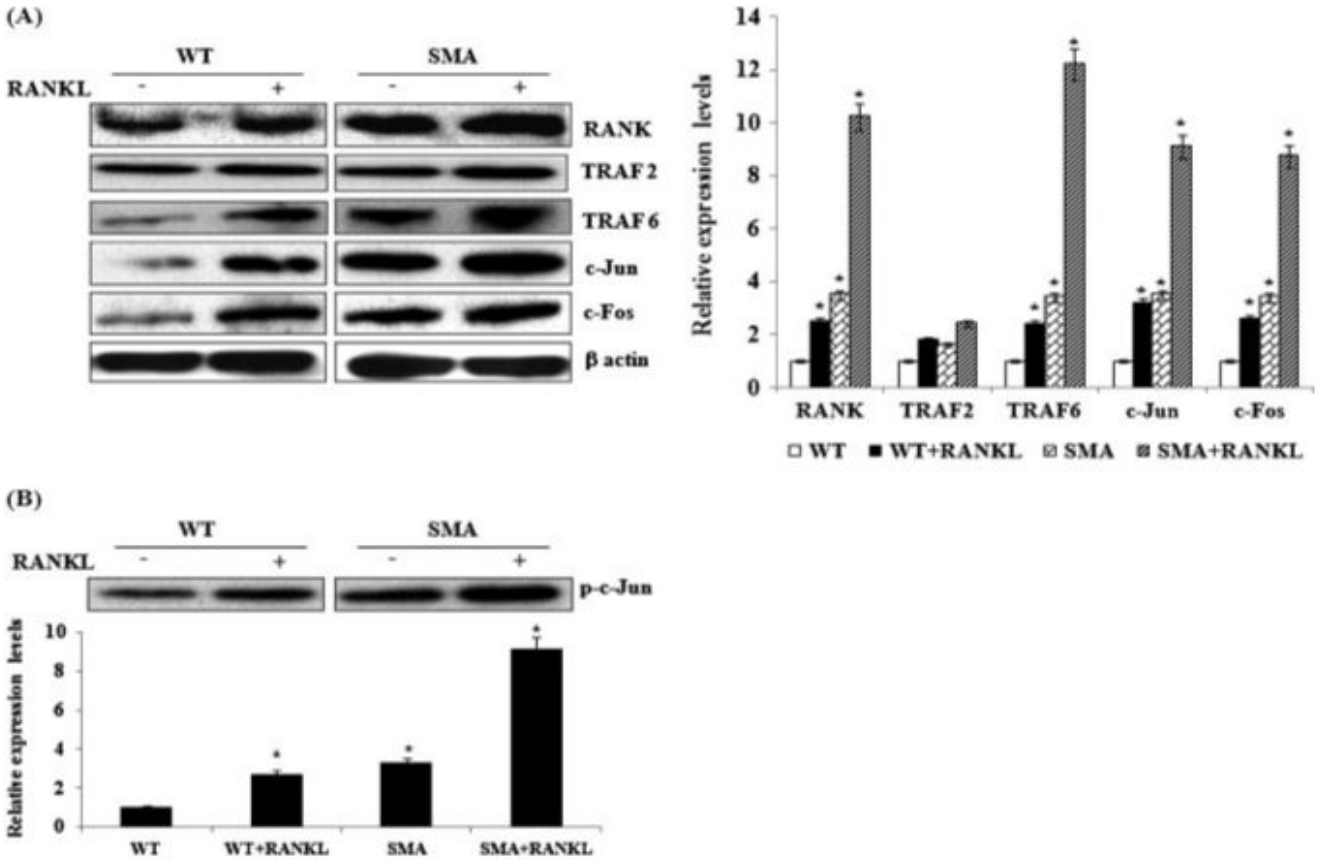

Figure 5.

Western blot analysis of RANK receptor signalling molecules during osteoclast differentiation. (A) WT and SMA mouse-derived bone marrow cells were cultured in the presence of 10 ng/ml M-CSF for 24 h. The non-adherent cells were cultured in the presence of M-CSF (10 ng/ml) and stimulated with or without RANKL (100 ng/ml) for 2 days. Total cell lysates obtained from these pre-osteoclast cells were subjected to Western blot analysis for RANK, TRAF2, TRAF6, c-Jun and c-Fos expression. *β*-actin expression levels were also analysed to normalize the protein loading onto the gels in all the samples. (B) p-c-Jun kinase activity in the pre-osteoclast cells derived from WT and SMA mice. Band intensities were quantified densitometrically using the NIH Image J program and relative expression levels were normalized for *β*-actin expression in all the samples analysed. The data represent three independent experiments ($n = 6$ mice; $p < 0.05$)